Published in final edited form as:
Kidney Int. 2011 April ; 79(8): 883–896. doi:10.1038/ki.2010.526.

PKCβ-induced Selective IRS1 Dysfunction and Insulin Resistance in Renal Glomeruli of Rodent Models of Diabetes and Obesity

Akira Mima, MD, PhD[1], **Yuzuru Ohshiro, MD, PhD**[1], **Munehiro Kitada, MD, PhD**[1], **Motonobu Matsumoto, PhD**[1], **Pedro Geraldes, PhD**[1], **Chenzhong Li, MD, PhD**[1], **Qian Li, MD, PhD**[1], **Gregory White, BS**[1], **Christopher Cahill, BS**[2], **Christian Rask-Madsen, PhD**[1], and **George L. King, MD**[1,*]

[1]Section of Vascular Cell Biology, Joslin Diabetes Center, Harvard Medical School, Boston, Massachusetts 02215

[2]Section of Islet Cell and Regenerative Biology, Joslin Diabetes Center, Harvard Medical School, Boston, Massachusetts 02215

Abstract

Insulin resistance has been associated with the progression of chronic kidney disease in both diabetes and obesity. This study characterizes insulin signaling in renal tubules and glomeruli in insulin resistant and diabetic states.

Insulin-induced phosphorylation of insulin receptor substrate-1 (IRS1), Akt, endothelial nitric oxide (eNOS), and glycogen synthase kinase 3α (GSK3α) were selectively inhibited in the glomeruli but not in the renal tubules of both streptozotocin (STZ)-diabetic and Zucker fatty, insulin resistant rats compared to non-diabetic and Zucker lean rats. Protein levels, but not the mRNA expression, of IRS1 were decreased only in the glomeruli of STZ-diabetic rats and increased its association with ubiquitination. Protein kinase C (PKC) β isoform inhibitor, ruboxistaurin (RBX), treatment enhanced insulin actions and elevated IRS1 expression. In glomerular endothelial cells, high glucose inhibited phosphorylation of Akt, eNOS and GSK3α, decreased IRS1 protein expression and increased association with ubiquitination. Overexpression of IRS1 or the addition of RBX reversed the inhibitory effects of high glucose.

Selective inhibition of the IRS1/PI3K/Akt pathway and insulin activation of eNOS and GSK3α in the glomeruli in diabetes and insulin resistance is partly due to increased IRS1 degradation and PKCβ activation. The loss of insulin's effect on endothelial eNOS and GSK3α activation may contribute to the glomeropathy observed in diabetes and obesity.

Keywords

diabetic nephropathy; insulin resistance; obesity; insulin receptor substrate-1; protein kinase C β

[*]Address reprint requests to: George L. King, MD, Dianne Nunnally Hoppes Laboratory for Diabetes Complications, Section of Vascular Cell Biology & Complications Joslin Diabetes Center, One Joslin Place, Boston, MA 02215, Tel: 617-309-2622 Fax: 617-309-2637, George.king@joslin.harvard.edu.

Disclosure: All the authors declared no competing interests.

Introduction

Diabetic nephropathy is the most common cause of chronic kidney disease (CKD) and end-stage renal disease (1-3). Insulin resistance, observed in both diabetes and obesity, has been associated with increased risks of renal dysfunction and CKD (4). However, a comprehensive and comparative characterization of insulin signaling in renal glomeruli and tubules has not been reported in these diseases.

Physiological studies have shown that renal tissues are responsive to insulin, specifically in the renal tubules affecting sodium uptake and glucose metabolism (5, 6). Insulin's effect on renal sodium re-absorption has been reported to be unaffected in diabetes or insulin resistance, manifested by increased fluid retention in diabetic patients after the initiation or intensification of insulin therapy(7). However, systemic insulin resistance has been associated with the progression of nephropathy in type 1 diabetic patients (8, 9). Thus, insulin may have actions in the glomeruli and the proximal tubules. A potential site of insulin's glomerular action is the endothelial cells, regulating eNOS and altering nitric oxide (NO) production and actions (10). The role of NO and eNOS in renal function and pathology is significant since eNOS null mice exhibit glomerular and peritubular capillary endothelium injury with progressive renal disease (11, 12). Insulin can increase NO production by increasing eNOS actions in endothelial cells (13), which can be impaired in insulin resistant or diabetic animals (14, 15). NO production has been reported to be decreased in the renal cortex of diabetic(16) and Zucker fatty (ZF) rats(17) and patients with CKD(18).

This study characterized insulin signaling and actions in renal glomeruli and tubules of rat models of diabetes with insulin deficiency and insulin resistance due to obesity. The mechanisms for the selective loss of insulin glomerular actions were further studied in cultured rat glomerular endothelial cells (RGEC).

Results

Physiological characteristics of the experimental groups

Increases in blood glucose by 3.9- ± 0.5-fold, kidney weight by 1.6- ± 0.2-fold and albuminuria by 24±7-fold were observed in diabetic rats compared to control SD rats. After 8 weeks of diabetes, body weight in diabetic SD rats were less than the control SD rat group by 39±15% (P<0.001, Table 2), although all the final weights of the diabetic rats were higher than their weights at the initiation of the study. Body weights of ZF rats were significantly greater than Zucker lean (ZL) rats by 1.6- ± 0.7-fold (P<0.001, Table 2).

Renal histology in experimental groups

Mesangial matrix expansion was prominent in diabetic rats (control SD rats; 3.1±0.6% vs. diabetic SD rats; 5.5±2%, P<0.05, Figs. 1A-B). Area in the glomeruli stained for type IV collagen was also increased in diabetic rats compared to control SD rats (control SD rats; 2.9±0.9% vs. diabetic SD rats; 4.9±0.7%, respectively (P<0.05) (Figs. 1A and C).

Insulin's effect on the phosphorylation of Akt and Erk/MAPK

In the glomeruli, insulin stimulated p-Akt by at least 18±3-fold vs. control SD or ZL rats. In diabetic SD and ZF rats, insulin-induced p-Akt levels were inhibited by 51±4% (P<0.001, Fig. 2A) and 69±9% (P<0.001, Fig. 2B) compared with non-diabetic SD control and ZL rats, respectively. In contrast, insulin increased p-Akt in the tubules by 15- ± 3-fold to 25- ± 4-fold in all groups (P<0.001, Figs. 2A-B), which were unaffected by diabetes.

Immunohistochemistry indicated that the number of p-Akt positive cells in the glomeruli of control SD rats treated with insulin was increased significantly by 9.1±1.6-fold when compared to control SD rats without insulin. In diabetic SD rats treated with insulin, the number of p-Akt positive cells were decreased by 42±10% when compared to control SD rats with insulin (P<0.05, Figs. 2C-D).

Insulin increased Erk1/2 phosphorylation (p-Erk1/2) levels in both the glomeruli by up to 5.8- ± 0.2-fold (P<0.001, Figs. 2E-F) and the tubules by up to 7.6±0.4-fold P<0.001, Figs. 2E-F) when comparing STZ-diabetic SD and ZF rats to their respective controls. Moreover, the levels of phosphorylation peaked similarly (88±5 to 95±3%; p-Erk1/2/Erk1/2, Figs. 2E-F). Basal levels of p-Erk1/2 were increased in both glomeruli and tubules of diabetic SD rats (42±3% and 27±1%, respectively; p-Erk1/2/Erk1/2, P<0.001, Figs. 2E-F) and ZF rats (40±1% and 23±1%, respectively; p-Erk1/2/Erk1/2, P<0.05, Figs. 2E-F) as compared to non-diabetic and ZL rats.

In addition, we have checked the insulin's effect on renal tubular cell line (RPTEC), as in the case *in vivo*, insulin-induced p-Erk1/2 and p-Akt were not inhibited in high glucose condition (Supplementary Figs. 1E-F).

Phosphorylation of eNOS and GSK3α

Insulin increased p-eNOS in the glomeruli of SD non-diabetic and ZL rats by 6.4- ± 2.9-fold and 13- ± 3-fold, respectively. However, insulin's effect to increase p-eNOS was reduced by 15±6% (P<0.05, Fig. 3A) in STZ-diabetic SD compared with non-diabetic rats and was reduced by 68±1% in ZF compared with ZL rats (P<0.001, Fig. 3B).

To confirm the activation of PI3K/Akt is selectively inhibited in the glomeruli, we investigated insulin-stimulated phosphorylation of GSK3α (p-GSK3α), another target of insulin signaling induced by the activation of the IRS/PI3K pathway(19). Insulin increased p-GSK3α in the glomeruli of all rat groups by at least 7.6- ± 1.2-fold. Similar to eNOS activation, GSK3α phosphorylation was reduced by 23±3% in STZ-diabetic rats and 62±3% in ZF rats as compared with control SD and ZL rats, respectively (P<0.001, Figs. 3C-D). In contrast, insulin induced increases of p-GSK3α in the tubules were comparable in control and diabetic rats by 7.9- ± 0.5-fold to 10±1-fold (P<0.001, Figs. 3C-D). Lastly, GSK3β phosphorylation induced by insulin was reduced by 57±3% in STZ-diabetic SD rats and 53±1% in ZF rats as compared with control SD and ZL rats, respectively (P<0.001, Figs. 3E-F).

Characterization of mRNA and protein levels of IRS1/2

To identify possible mechanisms of insulin resistance on the activation of Akt/eNOS in the renal glomeruli, the protein and mRNA levels of IRS1/2 were assessed. Protein levels of IRS1, measured by immunoblot analysis, in the glomeruli of STZ-diabetic SD rats were reduced by 54±9% as compared with controls (P<0.05, Fig. 4A). In contrast, IRS1 protein levels in the glomeruli from ZF rats were not changed vs. ZL rats. No significant differences in the expression of mRNA levels of IRS1/2 and IRS2 protein levels in the glomeruli and tubules were observed in all four groups of rats (Fig. 4B-C).

Studies using immunohistochemistry showed that the number of IRS1 positive cells was significantly decreased in STZ-diabetic SD rats by 36±6% when compared to control SD rats (P<0.05, Figs. 4D-E).

Evaluation of insulin receptors and IRS1/2 activation

Insulin-induced tyrosine phosphorylation of IR in both glomeruli and tubules were increased by 8.5- ± 0.1-fold to 16- ± 1-fold and 7.8- ± 0.4-fold to 13- ± 3-fold, respectively (P<0.001, Supplementary Figs. 1A-B) and did not differ significantly when compared to their respective controls. In contrast, tyrosine phosphorylation of IRS1 was significantly reduced in the glomeruli of diabetic and ZF rats by 21±2% and 64±1% compared with control SD and ZL rats, respectively (P<0.001, Figs. 4F-G). Insulin increased IRS1 tyrosine phosphorylation in the tubules by 5.5- ± 0.5-fold to 23±2-fold, and no differences were observed between STZ-diabetic SD and ZF rats and their controls (P<0.001, Figs. 4F-G).

Association of ubiquitin with IRS1/2 in the glomeruli

The results suggest that the decreases of IRS1 in the diabetic SD rats are due to changes in the degradation of IRS1. The association of IRS1/2 with ubiquitin was evaluated by immunoprecipitation studies(20). Figure 4H showed that there was a significant increase by 2.3- ± 0.7-fold in the association of ubiquitin with IRS1 in the glomeruli of diabetic SD rats compared with non-diabetic control, (P<0.001). No increases in association between ubiquitin and IRS2 were observed in the glomeruli of diabetic vs. control SD rats. In addition, no changes in the association of IRS1/2 with ubiquitin were observed in the glomeruli of ZL vs. ZF rats (Fig. 4I).

NF-κB activation in kidney

Previous reports have indicated that GSK3α/β phosphorylation is decreased in the renal cortex and associated with increases in NF-κB activity(21, 22). Thus, we evaluated the activation of NF-κB in kidney. In the glomeruli of diabetic SD rats and ZF rats, NF-κB activation was increased by 6.4±0.2-fold in the glomeruli of diabetic SD rats when compared to control SD rats and by 7.8±0.9-fold in the glomeruli of ZF rats when compared to ZL rats (P<0.001, Fig. 5A). However, no increases were observed in the tubules of diabetic SD rats and ZF rats. Similar to immunoblot study, NF-κB binding assay only exhibited increases in the glomeruli of diabetic SD rats and ZF rats when compared to control SD rats and ZL rats (5.7±0.8-fold and 7.5±0.9-fold, respectively (P<0.001, Fig. 5B).

Effects of RBX on insulin-induced Akt, eNOS and GSKα phosphorylation

We have previously reported that activation of PKC, especially PKCβ, inhibited insulin-stimulated p-Akt and p-eNOS(15). Therefore, we evaluated whether inhibition by RBX can decrease insulin resistance in the glomeruli of diabetic SD and ZF rats. RBX treatment did not affect insulin-induced phosphorylation of Akt or its actions in the glomeruli of control SD rats and ZL rats. In contrast, RBX treatment partially normalized Akt phosphorylation by 67±14% and by 43±12%, respectively (P<0.001, P<0.05, Figs. 5C-D) in the glomeruli of diabetic SD rats and ZF rats. Treatment with RBX also normalized eNOS phosphorylation by 122±20% and by 144±48%, respectively (P<0.001, Figs. 5E-F) and GSK3α phosphorylation by 68±4% and by 136±10%, respectively (P<0.001, Figs. 5G-H) in diabetic SD and ZF rats. In addition, RBX treatment partially normalized insulin-induced levels of p-Erk1/2 and basal p-Erk1/2 (Supplementary Fig. 1C).

Effect of RBX on IRS1 function and NO synthesis

In the glomeruli of diabetic SD rats and ZF rats, RBX partially normalized insulin induced tyrosine phosphorylation of IRS1 by 165±21% and by 164±11%, respectively (P<0.001, Figs. 6A-B). Moreover, RBX decreased the degradation of IRS1 by 26±11% (P<0.001, Fig. 6A) and its association with ubiquitin by 35±7% (P<0.001, Fig. 6C) in the glomeruli of diabetic SD rats compared to diabetic SD rats. NO release induced by insulin in the isolated glomeruli of diabetic SD rats and ZF rats were reduced by 40±6% and by 41±5%,

respectively (P<0.001, Figs. 6D-E) compared to control and ZL rats. In the isolated glomeruli from diabetic SD rats and ZF rats, RBX treatment improved insulin-induced NO release by 30±10% and by 31±11%, respectively (P<0.05, Figs. 6D-E).

Effect of glucose levels on IRS1 expression and ubiquitination

To investigate whether hyperglycemia is responsible for the increase in IRS1 degradation, we studied the effect of high glucose on IRS mRNA and protein levels in RGEC, cultured for 72 hours, in the presence of low (5.5mM) and high (25mM) glucose levels. Levels of IRS1 and IRS2 mRNA and the protein levels of IRS2 were not changed during the experiments (Fig. 7A).

The protein levels of IRS1 decreased in high glucose condition after 48 and 72 hours of incubation by 21±2% and 30±1% compared with basal, respectively; (P<0.05, P<0.001, Fig. 7B). Similar to the *in vivo* condition, polyubiquitination for IRS1 in RGEC was increased by 1.7- ± 0.2-fold when cells were incubated with high glucose for 72 hours compared with low glucose condition (P<0.001, Fig. 7C). No difference for IRS2 immunoreactive band associated with ubiquitin between control and diabetic rats was detected (Fig. 7C).

We also checked the differences of insulin receptor and IRS expression amongst the glomerular cell types. In podocytes, both insulin receptor and IRS1expression were higher than other cells (insulin receptor/actin; 85±13% in podocytes, 74±10% in mesangial cells and 80±15% in RGEC, respectively (IRS/actin; 87±11% in podocytes, 70±11% in mesangial cells and 82±14% in RGEC) (P<0.05) (Supplementary Fig. 1G).

Effect of glucose and the overexpression of IRS1 on insulin signaling in RGEC

Since eNOS is selectively expressed in the endothelial cells and inhibited by diabetes, we characterized the direct effect of glucose levels on insulin signaling and activation of eNOS in RGEC. As shown in Figures 6D-F, insulin at 5.5mM glucose significantly increased p–Akt (Ser473), p-eNOS (Ser1177), and p-Erk1/2 by 3-4-fold (P<0.001) with maximum effects observed at 30, 30 and 15 minutes after the addition of insulin, respectively.

Infection with Ad-IRS1 increased IRS1 protein expression similarly in low and high glucose levels with 9.1- ± 1.9-fold and 9.4- ± 0.3-fold, respectively, (P<0.001, Supplementary Fig. 1C). Insulin increased p-Akt (Ser473)/Akt to 91±2% of total Akt in Ad-GFP infected cells (Fig. 7G), which were not different from non-infected RGEC (95±2% of total Akt protein, Fig. 7D). Infection of Ad-IRS1 increased basal p-Akt/Akt to 74±1% of total Akt. Insulin still significantly increased p-Akt in Ad-IRS1 infected cells; although the maximum did not change between Ad-GFP vs. Ad-IRS1 infected cells. In RGEC cultured in high glucose, the maximal stimulation of p-Akt in control or Ad-GFP infected cells showed a 15±3% inhibition compared to low glucose condition (P<0.05). The infection of Ad-IRS1 in RGEC reversed the loss of insulin's activation of p-Akt in RGEC incubated in high glucose conditions (Fig. 7G) without infection with Ad-IRS1. RGEC, incubated without insulin but with Ad-IRS1 infection had elevated basal p-eNOS levels (Fig. 7H). Lastly, insulin's effect on p-GSK3α was inhibited by 17±2% in RGEC incubated with high glucose as compared to low glucose conditions (P<0.001). Overexpression of Ad-IRS1 in RGEC totally normalized the maximum responses per p-GSK3α induced by insulin in high glucose conditions (Fig. 7I).

Effect of antioxidant, PKCβ inhibitor and proteosome inhibitor on RGEC

To characterize the possible role of PKC activation in RGEC, we examined the effects of GFX, a general PKC inhibitor or RBX, in RGEC. In RGEC cultured with high level of glucose, insulin's activation of p-Akt was inhibited, compared to low glucose condition

(P<0.001). Addition of GFX and RBX reversed the inhibitory effect of high glucose on p-Akt activation by 32±2% and by 17±2%, respectively (P<0.05). The addition of NAC, an antioxidant, also partially normalized this inhibition by 30±4% (P<0.05, Fig. 8A). Similarly, inhibitions of p-eNOS and p-GSK were also partially normalized by NAC, GFX or RBX (P<0.05, Figs. 8B-C). Next, we tested the effect of NAC, GFX, RBX and proteasome inhibitor, MG132 on proteasomal IRS1 degradation in RGEC. When the cells were incubated with high glucose for 72 hours, IRS1 protein levels in RGEC were decreased by 30±2%. NAC, GFX, RBX and MG132 significantly increased IRS1 proteins by 51±7%, 39±3%, 12±5% and 54±4%, respectively (Fig. 8D). For NO production in RGEC, insulin induced its production by 4.9- ± 0.7-fold. When incubated with high glucose, NO release was inhibited by 45±11% compared with low glucose condition (P<0.001, Fig. 8E). NAC, GFX and RBX increased NO production in RGEC exposed to high glucose level by 41±8%, 40±7% and 23±7%, respectively (P<0.05, Fig. 8E).

Discussion

This is the first comparative analysis of insulin signaling and cellular actions between renal glomeruli and tubules in control, insulin resistant and diabetic states. The results demonstrated that the renal tubules are protected from the loss of insulin action as a consequence of metabolic abnormalities induced by insulin resistance or diabetes. In contrast, insulin signaling and actions in the renal glomeruli are significantly inhibited in a selective manner, similar to the endothelium of all the other vascular tissues exposed to insulin resistance and diabetes (23, 24). Our findings of the selective loss of insulin action in the glomeruli but not in the tubules in both diabetes and insulin resistance has suggested a biochemical explanation for the glomerular pathologies shared by both of these pathological conditions (25, 26).

Resistance to insulin signaling and actions in the renal glomeruli is also selective for the activation of the IRS1/PI3K/Akt cascade; whereas the activation of the Erk/MAPK pathway by insulin remained fully active. This pattern of selective loss of insulin signaling in insulin resistant and diabetic states has been reported in many vascular beds, such as in the microvessels from adipose tissues and the aorta(13, 24). The diminution of eNOS activation induced by insulin suggests that the presence of glomeruli endothelial dysfunction and consistent with previous reports regarding decreasing NO production in the renal cortex of ZF rats and diabetic rodents (16, 17). The loss of insulin-induced eNOS activation and endothelial dysfunction in the glomeruli can contribute to changes in glomerular blood flow and loss of antioxidative and inflammatory actions of NO (12). Our results have also shown for the first time that there is also a parallel selective loss of insulin's inhibitory actions on GSK3α, limited to the glomeruli. Our data has demonstrated that this decrease in GSK3α phosphorylation is limited to the glomeruli and is partially related to the loss of insulin action, which is known to inhibit GSK3α activities by increasing its phosphorylation (19). The increases in GSK3α activity in the glomeruli can be equally important as the diminution of eNOS activation since GSK3α can regulate multiple critical actions in renal cells (27, 28), such as increases in oxidative stress via the activation of NF-κB and regulation of endothelial cell (29) and podocyte apoptosis via Wnt signaling (26, 30).

For Erk1/2 phosphorylation, the basal levels are increased in both diabetes and insulin resistance, which is consistent with previous reports (24, 31, 32). The increase of basal p-Erk in these pathological states is probably due to the activation of PKC (33) which is known to increase MAPK (15). Insulin-induced increased ratio of p-Erk in diabetic SD rats and ZF rats are decreased because the basal p-Erk level is increased. However, their maximal effects induced by insulin are similar in control and diabetic mice (24).

In diabetes, our results clearly suggest that hyperglycemia can induce a decrease in the protein level of IRS1, selectively, but not IRS2, in parallel with the loss of insulin action. The suggestion of enhanced degradation of IRS1 induced by hyperglycemia is supported by the increased association of polyubiquitination with IRS1, which was observed both in the glomeruli of diabetic rats and RGEC exposed to high concentrations of glucose. These findings indicate that hyperglycemia by an unknown mechanism increases IRS1 being targeted for proteasomal degradation.

Several mechanisms, such as the activation of PKC, have been identified to induce the selective inhibition of the IRS/PI3K/Akt pathway of insulin in the endothelial cells (15). The selective loss of IRS1 but not IRS2 is interesting, but has also been reported in macrophages and adipocytes in association with diabetes (34, 35). The potential mechanism for the selective loss of insulin's activation of IRS/PI3K/Akt/eNOS pathways appears to be the activation of PKC, possibly by the β isoform. The results indicated that hyperglycemia activated several PKC isoforms, including β to selectively inhibit the IRS/PI3K pathway resulting in the loss of eNOS and GSK3α actions. The target of PKC activation could be IRS1, which has been reported to be phosphorylated by PMA in non-vascular cells (36). The finding that the inhibition of PKCβ can improve glomerular endothelial function and insulin actions is consistent with previous reports of RBX being able to improve endothelial dysfunction in diabetes and insulin resistant states (13, 15).

Like diabetes, insulin resistance can also induce the selective loss of insulin action through the IRS/PI3K/Akt pathway (37). However, the mechanism of this selective loss of insulin action in the glomeruli by insulin resistance appears to be different from diabetes since no decreases in IRS1 protein or mRNA were found. This lack of change of IRS1 protein in the glomeruli and endothelial cells is consistent with other vascular beds that exhibit endothelial dysfunction (15, 36, 38). In obesity, free fatty acid is known to be elevated and can activate PKC (39). Our results indicate that abnormal metabolic factors, such as hyperglycemia and free fatty acids, can induce selective insulin resistance in the renal glomeruli, probably due to different mechanisms between diabetes and obesity. The pathophysiological significance of the findings suggests that glomerular endothelial dysfunction alone will not cause glomerulopathy as observed in diabetes. This is reflected by the lack of significant pathologies in the renal glomeruli in the ZF insulin resistance rats and the reduced level of nephropathy in obese and insulin resistant population without diabetes. However, the contribution of glomerular endothelial dysfunction may contribute significantly to the initiation and progression of glomerular lesions in diabetes when it is combined with abnormalities in the Mesangial cells and podocytes.

In summary, these observations have identified glomeruli as the site of insulin resistance in diabetic, obese and other insulin resistant states. Further, these findings suggest that increasing IRS1 levels or inhibiting PKCβ action as a possible therapeutic target could prevent or improve renal function in diabetic and insulin resistant states.

Materials and Methods

Animal studies

All protocols for animal use were approved by the animal care committee of the Joslin Diabetes Center and were in accordance with the National Institutes of Health guidelines. We used age-matched male SD (Harlan, Indianapolis, IN) and ZF rats and their lean matched controls, ZL rats. Diabetes was induced in 6 wk old SD rats by a single intravenous (IV) injection of STZ (55mg/kg body weight, Sigma, St. Louis, MO) in 0.05mol/l citrate buffer (pH 4.5) or citrate buffer for controls. Blood glucose levels, determined two days after the injections by glucose analyzer (Yellow Spring Instruments, Yellow Springs, OH)

and levels >16.7 mmol/L, were defined as having diabetes. The rats were randomly divided into eight groups; Control, Control with the PKCβ-selective inhibitor RBX (LY333531) (Lilly, Indianapolis, IN) treatment, DM, DM with RBX treatment, ZL, ZL with RBX treatment, ZF, ZF with RBX treatment. RBX was given orally using mixed chow (5mg/kg body weight/day) from the age of 7-14 weeks. Rats were anesthetized with 100 mg/kg of sodium pentobarbital injected intraperitoneally 8 weeks after diabetes or at 14 weeks of age for ZF and ZL. Regular human insulin (10mU/g, Lilly) or diluents were injected into the inferior vena cava for studying insulin signaling and action. After ten minutes injection, kidneys were harvested and all the procedures were performed within thirty minutes.

Cell culture

Glomeruli were isolated from kidneys of SD rats at six weeks of age under sterile conditions. The digested glomeruli were filtered through a 100mm cell strainer (BD Biosciences, San Jose, CA) twice. After centrifugation, the cells were mixed with sheep anti-rat IgG beads (Invitrogen, Carlsbad, CA) coated with anti-ICAM2 antibody or with streptavidin-coupled beads (Invitrogen) with biotin anti-CD31 (BD Biosciences) at antibody concentration of 3μg for 1×10^7 beads in 1mL Dulbecco's modified Eagle's medium (DMEM) containing 0.1% BSA. After 1 hour, RGEC were isolated using a MPC-50 magnet (Dynal, Hamburg, Germany)(40). The cells were cultured in 10cm dishes pre-coated with rat collagen I (5mg/cm^2) (BD Biosciences) at 37°C in a humidified 5% CO_2 atmosphere. On days 5-7 after seeding, outgrowths of individual glomeruli were detached by trypsin-EDTA (Invitrogen) and were washed with DMEM and subsequently treated with 0.1% collagenase type I (Worthington, Lakewood, NJ) in DMEM containing 0.1% BSA at 37°C for 1 hour. Endothelial cell purity >90% was assessed by immunofluorescence staining with CD31.

Real-time PCR analysis

IRS1/2 mRNA were assayed by Real-time PCR and normalized to 18S rRNA as described previously(41) (Table1).

Data analysis

The data are expressed as mean ± SD. Comparison among more than two groups was performed by one-way ANOVA followed by the post hoc analysis with paired or unpaired *t* test to evaluate statistical significance between the two groups. Statistical significance was defined as $P<0.05$.

Additional methodology

Reagents; measurement of urinary albumin; isolation of glomeruli and tubules; mesangial cell, podocyte and RPTEC culture; adenoviral vector infection; immunoblot analysis; Quantification of NO; NF-κB activation; and immunohistochemistry are described in the Supplementary Methods.

Supplementary Material

Refer to Web version on PubMed Central for supplementary material.

Acknowledgments

This work is supported by a grant from the National Institutes of Health/NIDDK to G.L.K. (DK053105). A.M. is the recipient of a Research Fellowship (Manpei Suzuki Diabetes Foundation, Kanzawa Medical Research Foundation, NOVARTIS Foundation, Japan). This project has been supported by DERC P30DK036836.

References

1. Ferrannini E, Natali A, Bell P, et al. Insulin resistance and hypersecretion in obesity European Group for the Study of Insulin Resistance (EGIR). J Clin Invest. 1997; 100:1166–1173. [PubMed: 9303923]
2. Remuzzi G, Benigni A, Remuzzi A. Mechanisms of progression and regression of renal lesions of chronic nephropathies and diabetes. J Clin Invest. 2006; 116:288–296. [PubMed: 16453013]
3. The effect of intensive treatment of diabetes on the development and progression of long-term complications in insulin-dependent diabetes mellitus. The Diabetes Control and Complications Trial Research Group. N Engl J Med. 1993; 329:977–986. [PubMed: 8366922]
4. Kramer HJ, Saranathan A, Luke A, et al. Increasing body mass index and obesity in the incident ESRD population. J Am Soc Nephrol. 2006; 17:1453–1459. [PubMed: 16597682]
5. Feraille E, Carranza ML, Rousselot M, et al. Insulin enhances sodium sensitivity of Na-K-ATPase in isolated rat proximal convoluted tubule. Am J Physiol. 1994; 267:F55–62. [PubMed: 8048565]
6. Tiwari S, Riazi S, Ecelbarger CA. Insulin's impact on renal sodium transport and blood pressure in health, obesity, and diabetes. Am J Physiol Renal Physiol. 2007; 293:F974–984. [PubMed: 17686957]
7. Kalambokis GN, Tsatsoulis AA, Tsianos EV. The edematogenic properties of insulin. Am J Kidney Dis. 2004; 44:575–590. [PubMed: 15384008]
8. Orchard TJ, Chang YF, Ferrell RE, et al. Nephropathy in type 1 diabetes: a manifestation of insulin resistance and multiple genetic susceptibilities? Further evidence from the Pittsburgh Epidemiology of Diabetes Complication Study. Kidney Int. 2002; 62:963–970. [PubMed: 12164879]
9. Thorn LM, Forsblom C, Fagerudd J, et al. Metabolic syndrome in type 1 diabetes: association with diabetic nephropathy and glycemic control (the FinnDiane study). Diabetes Care. 2005; 28:2019–2024. [PubMed: 16043748]
10. Nakagawa T, Sato W, Glushakova O, et al. Diabetic endothelial nitric oxide synthase knockout mice develop advanced diabetic nephropathy. J Am Soc Nephrol. 2007; 18:539–550. [PubMed: 17202420]
11. Bachmann S, Mundel P. Nitric oxide in the kidney: synthesis, localization, and function. Am J Kidney Dis. 1994; 24:112–129. [PubMed: 7517625]
12. Nakayama T, Sato W, Kosugi T, et al. Endothelial injury due to eNOS deficiency accelerates the progression of chronic renal disease in the mouse. Am J Physiol Renal Physiol. 2009; 296:F317–327. [PubMed: 19036847]
13. Kuboki K, Jiang ZY, Takahara N, et al. Regulation of endothelial constitutive nitric oxide synthase gene expression in endothelial cells and in vivo: a specific vascular action of insulin. Circulation. 2000; 101:676–681. [PubMed: 10673261]
14. Bohlen HG. Protein kinase betaII in Zucker obese rats compromises oxygen and flow-mediated regulation of nitric oxide formation. Am J Physiol Heart Circ Physiol. 2004; 286:H492–497. [PubMed: 14715497]
15. Naruse K, Rask-Madsen C, Takahara N, et al. Activation of vascular protein kinase C-beta inhibits Akt-dependent endothelial nitric oxide synthase function in obesity-associated insulin resistance. Diabetes. 2006; 55:691–698. [PubMed: 16505232]
16. Erdely A, Freshour G, Maddox DA, et al. Renal disease in rats with type 2 diabetes is associated with decreased renal nitric oxide production. Diabetologia. 2004; 47:1672–1676. [PubMed: 15490111]
17. Trujillo J, Ramirez V, Perez J, et al. Renal protection by a soy diet in obese Zucker rats is associated with restoration of nitric oxide generation. Am J Physiol Renal Physiol. 2005; 288:F108–116. [PubMed: 15328066]
18. Schmidt RJ, Baylis C. Total nitric oxide production is low in patients with chronic renal disease. Kidney Int. 2000; 58:1261–1266. [PubMed: 10972689]
19. Cohen P, Frame S. The renaissance of GSK3. Nat Rev Mol Cell Biol. 2001; 2:769–776. [PubMed: 11584304]
20. Ciechanover A, Finley D, Varshavsky A. Ubiquitin dependence of selective protein degradation demonstrated in the mammalian cell cycle mutant ts85. Cell. 1984; 37:57–66. [PubMed: 6327060]

21. Gong R, Ge Y, Chen S, et al. Glycogen synthase kinase 3beta: a novel marker and modulator of inflammatory injury in chronic renal allograft disease. Am J Transplant. 2008; 8:1852–1863. [PubMed: 18786229]
22. Rao R, Hao CM, Breyer MD. Hypertonic stress activates glycogen synthase kinase 3beta-mediated apoptosis of renal medullary interstitial cells, suppressing an NFkappaB-driven cyclooxygenase-2-dependent survival pathway. J Biol Chem. 2004; 279:3949–3955. [PubMed: 14607840]
23. He Z, Opland DM, Way KJ, et al. Regulation of vascular endothelial growth factor expression and vascularization in the myocardium by insulin receptor and PI3K/Akt pathways in insulin resistance and ischemia. Arterioscler Thromb Vasc Biol. 2006; 26:787–793. [PubMed: 16469952]
24. Jiang ZY, Lin YW, Clemont A, et al. Characterization of selective resistance to insulin signaling in the vasculature of obese Zucker (fa/fa) rats. J Clin Invest. 1999; 104:447–457. [PubMed: 10449437]
25. Nerlich A, Schleicher E. Immunohistochemical localization of extracellular matrix components in human diabetic glomerular lesions. Am J Pathol. 1991; 139:889–899. [PubMed: 1928305]
26. Rea DJ, Heimbach JK, Grande JP, et al. Glomerular volume and renal histology in obese and non-obese living kidney donors. Kidney Int. 2006; 70:1636–1641. [PubMed: 16955108]
27. Boini KM, Amann K, Kempe D, et al. Proteinuria in mice expressing PKB/SGK-resistant GSK3. Am J Physiol Renal Physiol. 2009; 296:F153–159. [PubMed: 18987114]
28. Kuure S, Popsueva A, Jakobson M, et al. Glycogen synthase kinase-3 inactivation and stabilization of beta-catenin induce nephron differentiation in isolated mouse and rat kidney mesenchymes. J Am Soc Nephrol. 2007; 18:1130–1139. [PubMed: 17329570]
29. Messmer UK, Briner VA, Pfeilschifter J. Basic fibroblast growth factor selectively enhances TNF-alpha-induced apoptotic cell death in glomerular endothelial cells: effects on apoptotic signaling pathways. J Am Soc Nephrol. 2000; 11:2199–2211. [PubMed: 11095643]
30. Serra A, Romero R, Lopez D, et al. Renal injury in the extremely obese patients with normal renal function. Kidney Int. 2008; 73:947–955. [PubMed: 18216780]
31. Geraldes P, Hiraoka-Yamamoto J, Matsumoto M, et al. Activation of PKC-delta and SHP-1 by hyperglycemia causes vascular cell apoptosis and diabetic retinopathy. Nat Med. 2009; 15:1298–1306. [PubMed: 19881493]
32. Schauer IE, Knaub LA, Lloyd M, et al. CREB downregulation in vascular disease: a common response to cardiovascular risk. Arterioscler Thromb Vasc Biol. 30:733–741. [PubMed: 20150559]
33. Haneda M, Koya D, Kikkawa R. Cellular mechanisms in the development and progression of diabetic nephropathy: activation of the DAG-PKC-ERK pathway. Am J Kidney Dis. 2001; 38:S178–181. [PubMed: 11576950]
34. Rondinone CM, Wang LM, Lonnroth P, et al. Insulin receptor substrate (IRS) 1 is reduced and IRS-2 is the main docking protein for phosphatidylinositol 3-kinase in adipocytes from subjects with non-insulin-dependent diabetes mellitus. Proc Natl Acad Sci U S A. 1997; 94:4171–4175. [PubMed: 9108124]
35. Hartman ME, O'Connor JC, Godbout JP, et al. Insulin receptor substrate-2-dependent interleukin-4 signaling in macrophages is impaired in two models of type 2 diabetes mellitus. J Biol Chem. 2004; 279:28045–28050. [PubMed: 15123681]
36. Werner ED, Lee J, Hansen L, et al. Insulin resistance due to phosphorylation of insulin receptor substrate-1 at serine 302. J Biol Chem. 2004; 279:35298–35305. [PubMed: 15199052]
37. Dokken BB, Sloniger JA, Henriksen EJ. Acute selective glycogen synthase kinase-3 inhibition enhances insulin signaling in prediabetic insulin-resistant rat skeletal muscle. Am J Physiol Endocrinol Metab. 2005; 288:E1188–1194. [PubMed: 15671078]
38. Hirosumi J, Tuncman G, Chang L, et al. A central role for JNK in obesity and insulin resistance. Nature. 2002; 420:333–336. [PubMed: 12447443]
39. Steinberg HO, Tarshoby M, Monestel R, et al. Elevated circulating free fatty acid levels impair endothelium-dependent vasodilation. J Clin Invest. 1997; 100:1230–1239. [PubMed: 9276741]
40. Rops AL, van der Vlag J, Jacobs CW, et al. Isolation and characterization of conditionally immortalized mouse glomerular endothelial cell lines. Kidney Int. 2004; 66:2193–2201. [PubMed: 15569308]

41. Renstrom F, Buren J, Eriksson JW. Insulin receptor substrates-1 and -2 are both depleted but via different mechanisms after down-regulation of glucose transport in rat adipocytes. Endocrinology. 2005; 146:3044–3051. [PubMed: 15845625]

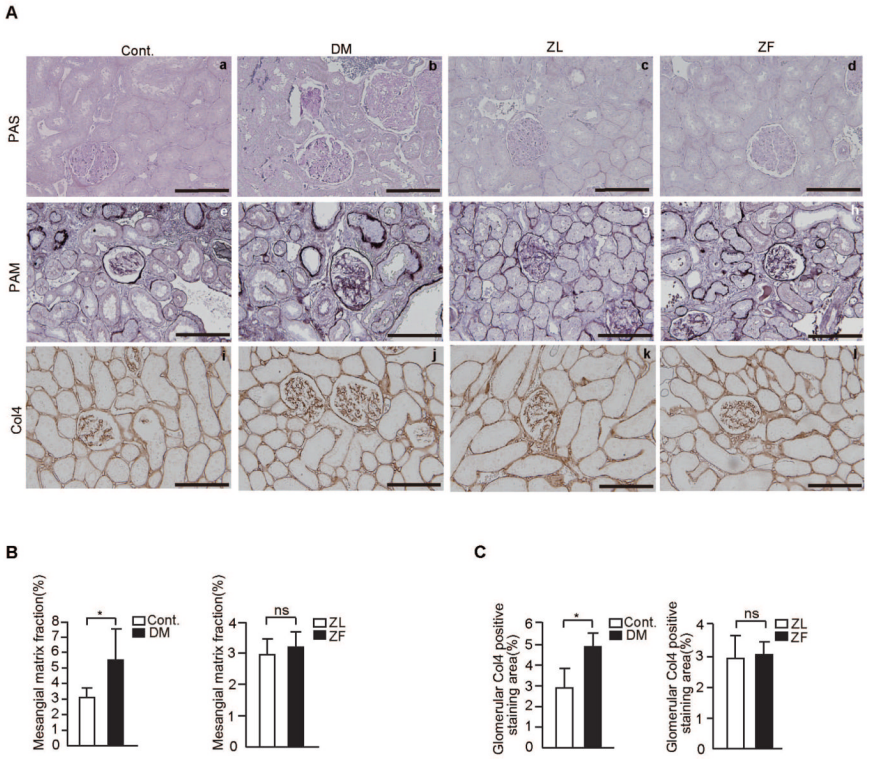

Figure 1. Renal morphology and immunohistochemical staining for type IV collagen in the experimental groups

A. Representative light microscopic appearance of glomeruli (PAS and PAM staining) and immunohistochemistry of Col4 for control rats (a, e, and i), STZ-induced diabetic SD rats, (b, f, and j), Zucker lean rats(c,g, and k), and Zucker fatty rats (d, h, and l). Bar = 100 μm. B. Morphometric analysis of PAM positive staining area. The glomerular PAM positive area was measured as described in materials and methods. n=6 in each group, **P*<0.05. C. Morphometric analysis of the glomerular expression of Col4. The glomerular staining area of Col4 was measured as described in materials and methods. n=6 in each group, **P*<0.05. The data are expressed as means ± SD. Cont.= control rats, DM=STZ-induced diabetic SD rats, ZL=Zucker lean rats, ZF=Zucker fatty rats, ns=not significant.

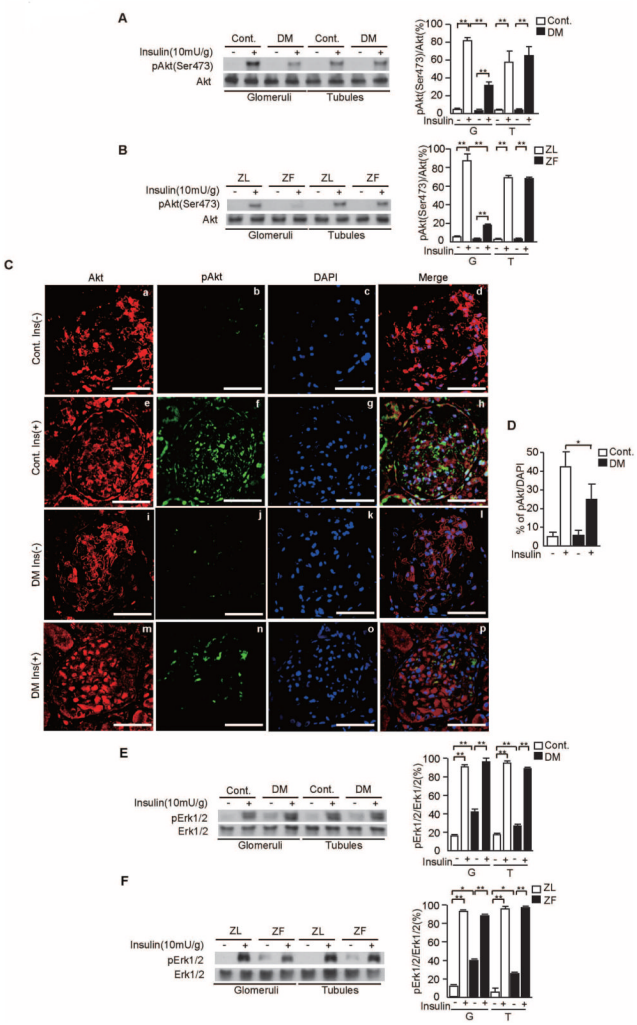

Figure 2. Insulin's effect on p-Akt and p-Erk1/2 in the glomeruli and tubules of SD and Zucker rats

A and B. Representative immunoblots of p-Akt from glomerular and tubular fractions. Data from three experiments were quantitated by densitometry. A) Cont. vs. DM, B) ZL vs. ZF, n=6 in each group, $^{**}P<0.001$.

C. Immunostaining for Akt (a, e, i, and m), p-Akt (b, f, j, and n), DAPI (c, g, k, and o), and merge images (d, h, i, and p) in the glomeruli of control rats without insulin, control rats with insulin, STZ-induced diabetic SD rats without insulin, and STZ-induced diabetic SD rats with insulin.

D. Percentage of p-Akt positive cells per DAPI. n=6 in each group, $^{*}P<0.05$.

E and F. Representative immunoblots of p-Erk1/2 from glomerular and tubular fractions. Data from three experiments were quantitated by densitometry. E) Cont. vs. DM, F) ZL vs. ZF, n=6 in each group, $^{*}P<0.05$, $^{**}P<0.001$. These data are expressed as means ± SD. Cont.= control rats, DM=STZ-induced diabetic SD rats, ZL=Zucker lean rats, ZF=Zucker fatty rats, G=glomeruli, T=tubules.

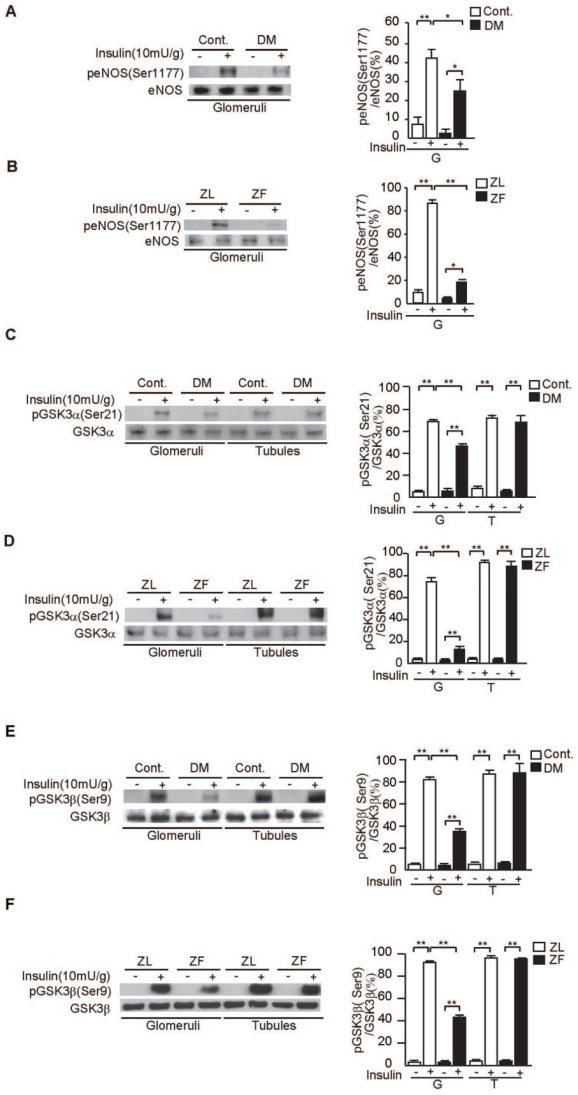

Figure 3. Insulin-induced p-eNOS and p-GSKα in the glomeruli and tubules of diabetic and control SD rats and ZL and ZF rats

A and B. Representative immunoblots of p-eNOS from glomerular proteins. Data from three experiments were quantitated by densitometry. A) Cont. vs. DM, B) ZL vs. ZF, n=6 in each group, *P<0.05, **P<0.001.

C and D. Representative immunoblots of p-GSKα from glomerular and tubular fractions. Data from three experiments were quantitated by densitometry. C) Cont. vs. DM, D) ZL vs. ZF, n=6 in each group, **P<0.001.

E and F. Representative immunoblots of p-GSKβ from glomerular and tubular fractions. Data from three experiments were quantitated by densitometry. E) Cont. vs. DM, F) ZL vs. ZF, n=6 in each group, **P<0.001. These data are expressed as means ± SD. Cont.= control rats, DM=STZ-induced diabetic SD rats, ZL=Zucker lean rats, ZF=Zucker fatty rats, G=glomeruli, T=tubules.

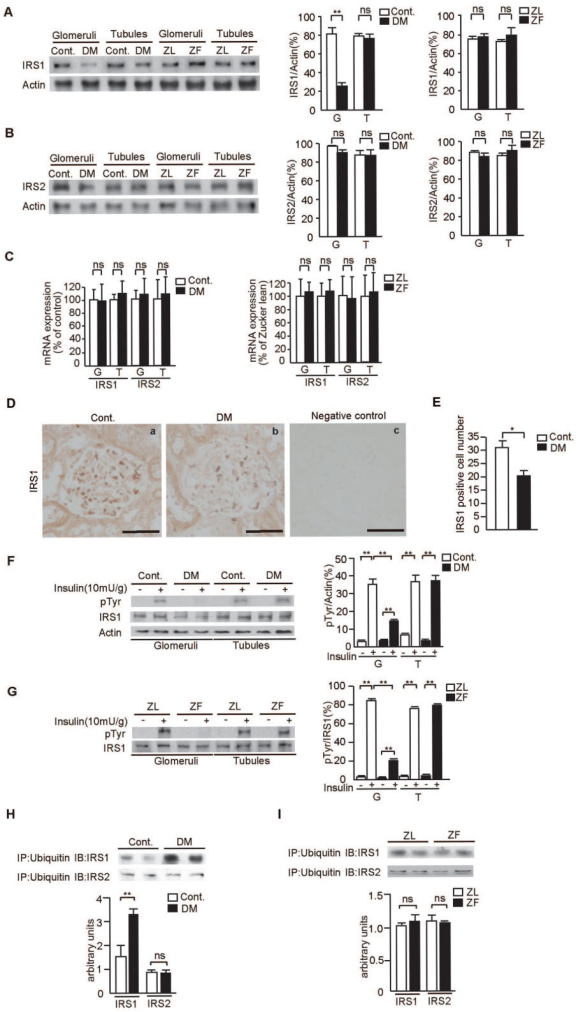

Figure 4. Expression of IRS1/2 proteins and mRNA levels and insulin's effect on the tyrosine phosphorylation IRS1 in the glomeruli and tubules

A and B. Representative immunoblots of IRS1 and IRS2 from glomerular and tubular fractions. Data from three experiments were quantitated by densitometry. A) IRS1, B) IRS2, n=6 in each group, $^{**}P<0.001$.

C. Glomerular and tubular fractions in diabetic and Zucker rats. mRNA expressions for IRS1/2 were measured by real time RT-PCR, n=6 in each group.

D. Immunostaining for IRS1 and representative pictures in control rats (a), STZ-induced diabetic SD rats (b), and Negative control (c). Bar = 50 μm.

E. Number of IRS1 positive-cells per glomerulus in control rats and STZ-induced diabetic SD rats. n=6 in each group, $^{*}P<0.05$.

F and G. Representative immunoblots of tyrosine phosphorylation of IRS1 from glomerular and tubular fractions. Solubilized glomeruli and tubular fractions were isolated and subjected to immunoprecipitation followed by immunoblotting. Data from three experiments were quantitated by densitometry. F) Cont. vs. DM, G) ZL vs. ZF, n=6 in each group, $^{**}P<0.001$.

H and I. Solubilized glomeruli fractions were immunoprecipitated with antibodies against ubiquitin and subsequently immunoblotted with anti-IRS1 or anti-IRS2 antibodies. Data from three experiments were quantitated by densitometry, n=6 in each group, $^{**}P<0.001$. These data are expressed as means ± SD. Cont.=control rats, DM=STZ-induced diabetic SD

rats, ZL=Zucker lean rats, ZF=Zucker fatty rats, G=glomeruli, T=tubules, ns=not significant.

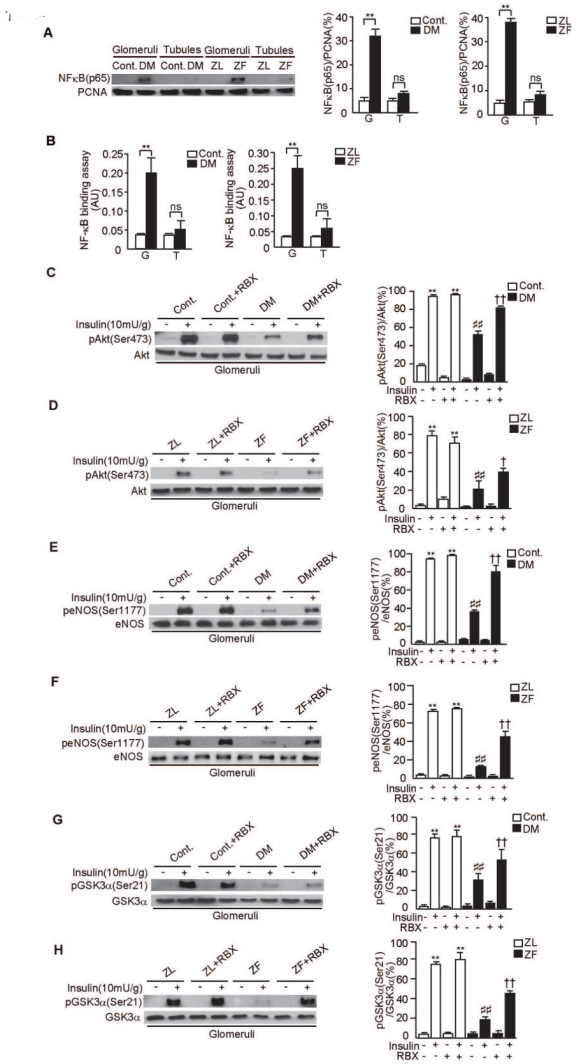

Figure 5. NF-κB activation and effect of RBX, PKCβ inhibitor on p-Akt, p-eNOS and p-GSK3α in the glomeruli of diabetic SD rats and ZF rats

A. Representative immunoblots of NF-κB (p65) from nuclear proteins of glomerular and tubular fractions. Data from three experiments were quantitated by densitometry. n=6 in each group, $^{**}P<0.001$.

B. Transcriptional binding activity assay of NF-κB in glomerular and tubular fractions. n=6 in each group, $^{**}P<0.001$.

C and D. Representative immunoblots of p-Akt from glomerular fractions. Data from three experiments were quantitated by densitometry. A) Cont. vs. Cont.+RBX vs. DM vs. DM +RBX, n=6 in Cont., Cont.+RBX and DM. n=5 in DM+RBX, $^{**}P<0.001$ vs. Cont./insulin(-)/RBX(-). $^{\#\#}P<0.001$ vs. Cont./insulin(+)/RBX(-). $^{\dagger\dagger}P<0.001$ vs. DM/insulin(+)/RBX(-). B) ZL vs. ZL+RBX vs. ZF vs. ZF+RBX n=6 in each group, $^{**}P<0.001$ vs. ZL/insulin(-)/RBX(-). $^{\#\#}P<0.001$ vs. ZL/insulin(+)/RBX(-). $^{\dagger}P<0.05$ vs. ZF/insulin(+)/RBX(-).

E and F. Representative immunoblots of p-eNOS from glomerular fractions. Data from three experiments were quantitated by densitometry. C) Cont. vs. Cont.+RBX vs. DM vs. DM +RBX, n=6 in Cont., Cont.+RBX and DM. n=5 in DM+RBX, $^{**}P<0.001$ vs. Cont./insulin(-)/RBX(-). $^{\#\#}P<0.001$ vs. Cont./insulin(+)/RBX(-). $^{\dagger\dagger}P<0.001$ vs. DM/insulin(+)/RBX(-). D) ZL vs. ZL+RBX vs. ZF vs. ZF+RBX n=6 in each group, $^{**}P<0.001$ vs. ZL/

insulin(-)/RBX(-). $^{\#\#}P<0.001$ vs. ZL/insulin(+)/RBX(-). $^{\dagger\dagger}P<0.001$ vs. ZF/insulin(+)/RBX(-).

G and H. Representative immunoblots of p-GSK3α from glomerular fractions. Data from three experiments were quantitated by densitometry. E) Cont. vs. Cont.+RBX vs. DM vs. DM+RBX, n=6 in Cont., Cont.+RBX and DM. n=5 in DM+RBX, $^{**}P<0.001$ vs. Cont./insulin(-)/RBX(-). $^{\#\#}P<0.001$ vs. Cont./insulin(+)/RBX(-). $^{\dagger\dagger}P<0.001$ vs. DM/insulin(+)/RBX(-). F) ZL vs. ZL+RBX vs. ZF vs. ZF+RBX n=6 in each group, $^{**}P<0.001$ vs. ZL/insulin(-)/RBX(-). $^{\#\#}P<0.001$ vs. ZL/insulin(+)/RBX(-). $^{\dagger\dagger}P<0.001$ vs. ZF/insulin(+)/RBX(-). These data are expressed as means ± SD. Cont.=control rats, Cont.+RBX=control rats treated with ruboxistaurin, DM=STZ-induced diabetic rats, DM+RBX=STZ-induced diabetic rats treated with ruboxistaurin, ZL=Zucker lean rats, ZL+RBX= Zucker lean rats treated with ruboxistaurin, ZF=Zucker fatty rats, ZF+RBX= Zucker fatty rats treated with ruboxistaurin, G=glomeruli, T=tubules, ns=not significant.

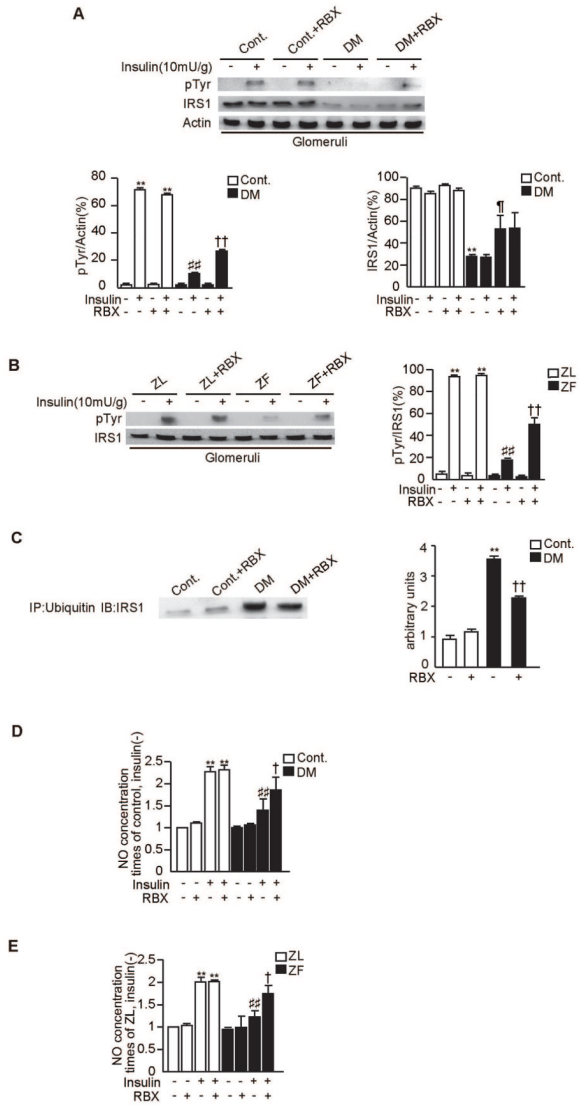

Figure 6. Effect of RBX on IRS1 and NO synthesis in the glomeruli of diabetic SD rats and ZF rats

A and B. Representative immunoblots of tyrosine phosphorylation of IRS1 from glomerular and tubular fractions. Solubilized glomeruli and tubular fractions were isolated and subjected to immunoprecipitation followed by immunoblotting. Data from three experiments were quantitated by densitometry. A) Cont. vs. Cont.+RBX vs. DM vs. DM+RBX, n=6 in Cont., Cont.+RBX and DM. n=5 in DM+RBX, $^{**}P<0.001$ vs. Cont./insulin(-)/RBX(-). $^{\#\#}P<0.001$ vs. Cont./insulin(+)/RBX(-). $^{\dagger\dagger}P<0.001$ vs. DM/insulin(+)/RBX(-). $^{\P}P<0.001$ vs. DM/insulin(-)/RBX(-). B) ZL vs. ZL+RBX vs. ZF vs. ZF+RBX n=6 in each group, $^{**}P<0.001$ vs. ZL/insulin(-)/RBX(-). $^{\#\#}P<0.001$ vs. ZL/insulin(+)/RBX(-). $^{\dagger\dagger}P<0.001$ vs. ZF/insulin(+)/RBX(-).

C. Solubilized glomeruli fractions were immunoprecipitated with antibodies against ubiquitin and subsequently immunoblotted with anti-IRS1 antibodies. Data from three experiments were quantitated by densitometry, n=6 in Cont., Cont.+RBX and DM. n=5 in DM+RBX, $^{**}P<0.001$ vs. Cont./RBX(-), $^{\dagger\dagger}P<0.001$ vs. DM/RBX(-).

D and E. The effect of RBX on NO synthesis in the glomeruli of diabetic SD rats and ZF rats. Isolated glomeruli from each group were incubated with insulin (100nM for 30

minutes). After homogenized and centrifuged, supernatant were collected. NO levels in the supernatant were measured with the Nitric Oxide Colorimeric Assay Kit. The results were derived from three separate experiments. D) $^{**}P<0.001$ vs. Cont./insulin(-)/RBX(-). $^{\#\#}P<0.001$ vs. Cont./insulin(+)/RBX(-). $^{\dagger}P<0.05$ vs. DM/insulin(+)/RBX(-). E) $^{**}P<0.001$ vs. ZL/insulin(-)/RBX(-). $^{\#\#}P<0.001$ vs. ZL/insulin(+)/RBX(-). $^{\dagger}P<0.05$ vs. ZF/insulin(+)/RBX(-).These data are expressed as means ± SD. Cont.=control rats, Cont.+RBX=control rats treated with ruboxistaurin, DM=STZ-induced diabetic rats, DM+RBX=STZ-induced diabetic rats treated with ruboxistaurin, ZL=Zucker lean rats, ZL+RBX= Zucker lean rats treated with ruboxistaurin, ZF=Zucker fatty rats, ZF+RBX= Zucker fatty rats treated with ruboxistaurin.

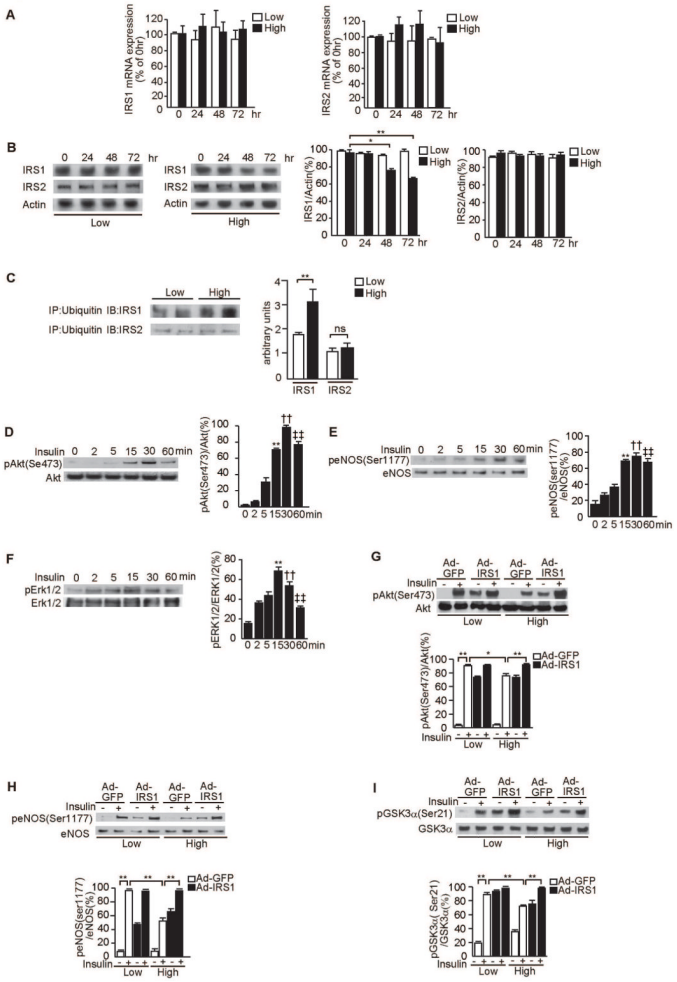

Figure 7. Effect of glucose levels on the association of IRS1/2 with ubiquitin and glucose levels on the activation of Akt, eNOS, Erk1/2 and overexpression of IRS1 in RGEC

A. Time course for the effect of high glucose levels on mRNA gene expression for IRS1 and IRS2 as measured by real time RT-PCR. RGEC were incubated with low glucose (5.5mM) or high glucose (20mM) as indicated. One of three independent experiments is shown.

B. Time course for the effect of high glucose levels on the protein expression of IRS1 and IRS2. RGEC were incubated with low glucose (5.5mM) or high glucose (20mM) as indicated. Data from three experiments were quantitated by densitometry. *P<0.05, **P<0.001.

C. Immunoprecipitation with antibodies against ubiquitin and subsequent immunoblotting analyses of the precipitate with anti-IRS1 or anti-IRS2 antibodies showed increased amounts of polyubiquinated IRS1 in high glucose condition. Data from three experiments were quantitated by densitometry. **P<0.001.

D–F. Time course of phosphorylation of Akt (D), eNOS (E) and Erk1/2 (F) by insulin. RGEC were incubated with 100nmol/l insulin for the indicated time. One of three independent experiments is shown. **P<0.001, ††P<0.001, ‡‡P<0.001 vs. 0 minutes.

G–I. Effect of IRS1 overexpression in RGEC on insulin–stimulated p-Akt (G), p-eNOS (H) and p-GSK3α (I). After RGEC were infected with Ad-GFP or with Ad-IRS1, cells were stimulated with insulin (100nmol/l, 30 minutes) as indicated in low glucose (5.5mM) or high glucose (20mM). One of three independent experiments is shown. *P<0.05, **P<0.001. These data are expressed as means ± SD.

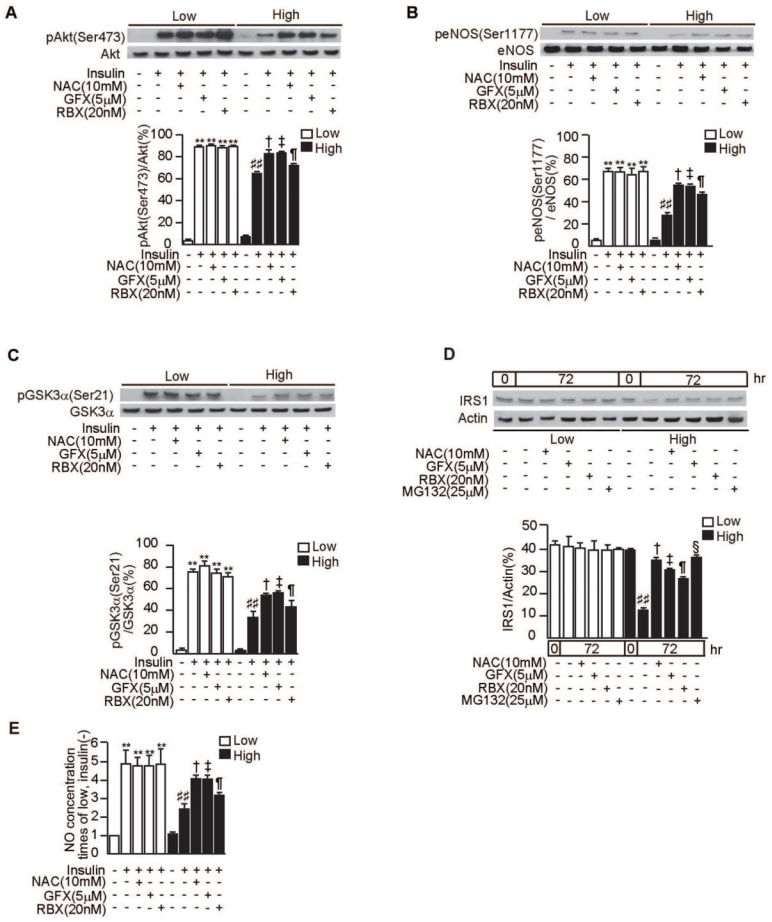

Figure 8. Effect of NAC, GFX, RBX and proteasome inhibitor on insulin signaling and degradation of IRS1 in RGEC

A-C. After 48 h of exposure to low glucose (5.5mM) or high glucose (20mM), RGEC were stimulated with insulin (100nmol/l, 30 minutes) with or without an antioxidant, N-Acetyl-L-Cystein (NAC, 10mM), or a PKC-specific inhibitor, GF109203X (GFX, 5μM), or PKCβ-specific inhibitor, LY333531 (RBX, 20nM). One of three independent experiments is shown. **P<0.001 vs. Low/insulin(-)/NAC(-)/GFX(-)/RBX(-). $^{\#\#}P$<0.001 vs. Low/insulin(+)/NAC(-)/GFX(-)/RBX(-). $^{\dagger}P$<0.05 vs. High/insulin(+)/NAC(-)/GFX(-)/RBX(-). $^{\ddagger}P$<0.05 vs. High/insulin(+)/NAC(-)/GFX(-)/RBX(-). $^{\P}P$<0.05 vs. High/insulin(+)/NAC(-)/GFX(-)/RBX(-). P-Akt(A), p-eNOS(B) and p-GSK3α (C).

D. RGEC were cultured in low glucose (5.5mM) or high glucose (20mM) media for 72 hours with or without NAC(10mM), GFX(5μM), RBX(20nM) or proteasome inhibitor, MG132(25μM). One of three independent experiments is shown. $^{\#\#}P$<0.001 vs. 0hr/High/NAC(-)/GFX(-)/RBX(-)/MG132(-). $^{\dagger}P$<0.001 vs. 72hr/High/NAC(-)/GFX(-)/RBX(-)/MG132(-). $^{\ddagger}P$<0.001 vs. 72hr/High/NAC(-)/GFX(-)/RBX(-)/MG132(-). $^{\P}P$<0.001 vs. 72hr/High/NAC(-)/GFX(-)/RBX(-)/MG132(-). $^{\S}P$<0.001 vs. 72hr/High/NAC(-)/GFX(-)/RBX(-)/MG132(-).

E. After 48 h of exposure to low glucose (5.5mM) or high glucose (20mM), RGEC were stimulated with insulin (100nmol/l, 30 minutes) with or without NAC (10mM), GFX (5μM), or RBX (20nM). NO levels in the culture media were measured with the Nitric Oxide Colorimeric Assay Kit. **P<0.001 vs. Low/insulin(-)/NAC(-)/GFX(-)/RBX(-). $^{\#\#}P$<0.001 vs. Low/insulin(+)/NAC(-)/GFX(-)/RBX(-). $^{\dagger}P$<0.05 vs. High/insulin(+)/NAC(-)/GFX(-)/

RBX(-). ‡P<0.05 vs. High/insulin(+)/NAC(-)/GFX(-)/RBX(-). ¶P<0.05 vs. High/insulin(+)/NAC(-)/GFX(-)/RBX(-). These data are expressed as means ± SD.

Table 1

Sequences of primers

Gene	Sequence (5′ – 3′)
18s rRNA	CGCGGTTCTATTTTGTTAGT; AGTCGGCATCGTTTATGGTC
IRS1	GCCAATCTTCATCCAGTTGC; CATCGTGAAGAAGGCATAGG
IRS2	CTACCCACTGAGCCCAAGAG; CCAGGGATGAAGCAGGACTA

Table 2

General characteristics of the experimental groups

	Cont.	Cont.+ RBX	DM	DM+ RBX	ZL	ZL+ RBX	ZF	ZF+ RBX
number	6	6	6	5	6	6	6	6
After 1 week								
Body weight (g)	165 ± 4	165±2	168 ± 8	166±1	188 ± 8	164±3	262± 23	261±12
Blood glucose (mg/dl)	98 ± 8	94±7	405±183 *	412±24 *	124 ± 9	100±13	159 ± 34	138±9
After 8 weeks								
Body weight (g)	527±45	541±56	320 ± 78 *	321±38 *	391±30	402±58	617± 23 †	621±36 †
Blood glucose (mg/dl)	106 ± 9	108±15	415 ± 50 *	456±66 *	114±24	130±16	157±46	170±49
Kidney weight (g)	2.3±0.1	2.2±0.2	3.7 ± 0.4 *	3.5±0.3 *	2.0±0.1	1.8±0.3	3.0±0.3 †	2.8±0.3
Albuminuria (mg/day)	0.2±0.1	0.2±0.1	4.7 ± 1.6 *	2.6±1.2 *#	0.1±0.1	0.2±0.1	0.6±0.3 ‡	0.4±0.2 ‡
Insulin (ng/ml)	2.4±0.5	2.5±0.4	0.2±0.1 *	0.2±0.1 *	2.9±0.5	2.8±0.4	42±3 †	43±5 †

Cont.=control rat, Cont.+RBX=control rat with ruboxistaurin (RBX) treatment DM=diabetic rat, DM+RBX=diabetic rat with RBX treatment, ZL=Zucker lean rat, ZL+RBX=Zucker lean rat with RBX treatment, ZF=Zucker fatty rat, ZF+RBX=Zucker fatty rat with RBX treatment.

The data are expressed as the means ± SD.

* $P<0.001$ vs. Cont.;

† $P<0.001$ vs. ZL;

‡ $P<0.05$ vs. ZL;

\# $P<0.05$ vs. DM